2023 IEEE 32nd Conference on Electrical Performance of Electronic Packaging and Systems (EPEPS) | 979-8-3503-1798-5/23/$31.00 ©2023 IEEE | DOI: 10.1109/EPEPS58208.2023.10314930

Wideband Complex Vector Fitting for Modeling Time Delay Variations in Passive Photonic Filters

Thijs Ullrick
IDLab
Ghent University - imec
Ghent, Belgium
Thijs.Ullrick@UGent.be

Dirk Deschrijver
IDLab
Ghent University - imec
Ghent, Belgium
Dirk.Deschrijver@UGent.be

Wim Bogaerts
Photonics Research Group
Ghent University - imec
Ghent, Belgium
Wim.Bogaerts@UGent.be

Tom Dhaene
IDLab
Ghent University - imec
Ghent, Belgium
Tom.Dhaene@UGent.be

***Abstract*—This paper presents a novel wideband baseband macromodeling framework tailored for the representation of linear and passive photonic filters. The proposed framework is able to efficiently estimate the baseband scattering representations of such filters as a function of the delay in the waveguides that control their center frequency. Notably, the macromodel allows for frequency and time-domain simulations at arbitrary optical carrier frequencies, making it especially well-suited for multi-wavelength system modeling and simulations. Although initially demonstrated in the context of photonic filters, a similar approach can be applied to baseband radio frequency (RF) systems. One application example is presented to demonstrate the flexibility and advantages of the proposed method.**

***Index Terms*—Photonic design automation (PDA), Vector fitting, parametric macromodeling, photonic integrated circuits.**

I. Introduction

BENEFITING from the combination of a very high index contrast and the compatibility with the CMOS fabrication technology, silicon photonic integrated circuits (PICs) are experiencing rapid growth in complexity, functionality, and integration scale. Since traditional electromagnetic (EM) modeling techniques are not suitable for directly simulating larger circuits, the PIC design flow is embracing electronic design automation (EDA) principles, favoring a more common circuit-level modeling approach [1]. This necessitates compact and efficient behavioral models that can substitute for the expensive EM simulations while ensuring a comparable accuracy [2].

A prominent subclass of photonic components are passive filters, such as ring resonators and Mach-Zehnder interferometers, whose behavior is best defined in the frequency-domain in terms of a scattering matrix. While these filters are usually characterized by various design parameters that shape the frequency response of the device, their center frequency is typically controlled by a single time delay. Consequently, a widely adopted approach among designers is to initially design the desired frequency response of the filter, and then create multiple instances of it, each with its own center frequency, to construct systems like a wavelength division multiplexing (WDM) filter bank.

This work has been supported by the Flemish Government under the 'Onderzoeksprogramma Artificiële Intelligentie (AI) Vlaanderen' and the 'Fonds Wetenschappelijk Onderzoek (FWO)' programs.

II. Methodology

Building upon the previous research conducted by Ye et al. [3], [4], this work presents a novel wideband baseband macromodeling framework tailored for the representation of linear and passive photonic filters whose center frequency is controlled by a single delay parameter, implemented by optical waveguides. In the following sections, the various steps involved in the proposed methodology are outlined.

A. Complex Vector Fitting (CVF)

The proposed parametric macromodeling framework in this work relies on the CVF algorithm [3] and starts from the scattering parameters of the photonic device under study, computed for a specific parameter configuration, typically chosen at the center of the design space. Let us assume that the scattering parameters of a photonic device have been acquired by means of EM simulations for a discrete set of frequencies within the bandwidth of interest: $\mathbf{S}(f_r)$ for $r = 1, ..., R$. The frequency response of the baseband equivalent system is then computed by shifting $\mathbf{S}(f_r)$ to baseband by substituting $f_i = f_r - f_c$, where f_c is the optical carrier frequency. Next, the baseband scattering parameters $\mathbf{S}_l(f_i)$ are fed to the CVF algorithm, which builds a pole-residue model in the form [3]

$$\mathbf{S}_l(s) = \sum_{k=0}^{K-1} \frac{\mathbf{R}_k}{s - p_k} + \mathbf{D} \tag{1}$$

where $s = j2\pi f$ is the Laplace variable, $\mathbf{R}_k \in \mathbb{C}^{n\times n}$ are the computed complex residues, p_k are the complex poles, and $\mathbf{D} \in \mathbb{R}^{n\times n}$ is a real matrix modeling the asymptotic response at high frequencies, where n is the total number of ports of the system under study. Starting from the rational model (1), it is possible to derive the corresponding state-space system analytically. This allows expressing the baseband scattering parameters $S_l(s)$ as a function the state-space matrices,

$$\mathbf{S}_l(s) = \mathbf{C}\left(s\mathbf{I}_m - \mathbf{A}\right)^{-1}\mathbf{B} + \mathbf{D} \tag{2}$$

where $m = nK$, $\mathbf{A} \in \mathbb{C}^{m\times m}$ is a diagonal matrix with the poles p_k at its non-zero entries, $\mathbf{B} \in \mathbb{R}^{m\times n}$ is a matrix that only has zeros or ones, $\mathbf{C} \in \mathbb{C}^{n\times m}$ is formed by horizontally stacking the residue matrices $\mathbf{R_k}$ and $\mathbf{D} \in \mathbb{R}^{n\times n}$ is the same matrix as in (1).

B. Wideband baseband macromodels

Prior to building the complex pole-residue model, it is necessary to select a specific value for the optical carrier frequency f_c in order to shift the photonic frequency response to baseband. If a new value of the carrier frequency is chosen, a new model in the form (2) must be computed. It is often not known upfront at which optical frequency(ies) the designers intend to perform simulations, so the modeling approach in Ye et al. [3] is not very flexible and it does not scale well for systems with multiple wavelength channels. In order to overcome these limitations, the model (2) is parameterized with respect to the optical carrier frequency by shifting its spectrum along the frequency axis by Δf_c

$$\mathbf{S}_w(f, \Delta f_c) = \mathbf{C}\left(j2\pi(f + \Delta f_c)\mathbf{I}_m - \mathbf{A}\right)^{-1}\mathbf{B} + \mathbf{D} \quad (3)$$

Expression (3) represents a new baseband equivalent system at center frequency $f_{cs} = f_c + \Delta f_c$ by means of the state-space matrices $(\mathbf{A} - j2\pi\Delta f_c\mathbf{I}_m)$, $\mathbf{B}$, $\mathbf{C}$ and $\mathbf{D}$. It should be noted that the new model can be directly obtained by shifting all the poles of the state-space model (2) computed at the optical carrier frequency f_c by $j2\pi\Delta f_c$. While the wideband state-space model (3) can be adopted for simulation at arbitrary optical carrier frequencies, it will be demonstrated that it can also be used to represent the variable delays in photonic filters.

C. Basic operating principles of optical filters

Most optical filters are based on interference of light with different delays. Incident light is separated over different paths, each with a different time delay Δt_i. At the end, the different parts are recombined by interference. Constructive interference will result in high transmission, and destructive interference will result in low transmission. The phase difference between two paths with a delay Δt is frequency dependent: $\Delta\phi = 2\pi f\Delta t$. Therefore, a time delay between two paths will translate into a frequency dependent interference. In most cases, the delays are integer multiples of a single delay Δt. The delays can be organized in a feed-forward or feed-back topology, or a mixture of both.

In integrated optical filters, the delays are implemented by routing light through waveguides. The delay Δt corresponds to

$$\Delta t = \frac{\Delta L \cdot n_g}{c_0} \quad (4)$$

where ΔL is the physical length of the waveguide, n_g is the group index of the waveguide and c_0 is the speed of light in vacuum. The phase delay $\Delta\phi$ in the delay line is

$$\Delta\phi = 2\pi\frac{f \cdot n_{eff} \cdot \Delta L}{c_0} \quad (5)$$

where n_{eff} is the effective index of the waveguide. The center frequency of an optical filter for the k^{th} interference order is given by

$$f_k = \frac{k \cdot c_0}{\Delta L \cdot n_{eff}(f_k)} \quad (6)$$

Rather than a single pass-band, the transmission spectrum selects multiple frequency or wavelength bands, separated by a free spectral range (FSR). This usually means that the operating range of the filter is limited to a single FSR. Tuning the center frequency of the filter affects both its magnitude and phase response. Nevertheless, if the center frequency is varied within one FSR, the resulting changes in magnitude and phase are relatively moderate.

D. Parametric delay modeling

Equation (6) indicates that the center frequency of the filter can be adjusted either by varying the length of the delay lines or by modifying their effective index, for instance, by altering the waveguide cross-sectional dimensions. In this work, the parameterization of the filter's response with respect to the center frequency is achieved in a similar manner as the parameterization with respect to the optical carrier frequency, i.e. by shifting the poles of the wideband macromodel by $j2\pi\Delta f_k$. However, in order to also accurately represent the filter's phase response, each scattering parameter of the wideband macromodel must be corrected with an additional phase delay. This is achieved by multiplying the elements of the residue matrices $\mathbf{R}_{k(ij)}$ and the elements of the asymptotic response matrix $\mathbf{D}_{(ij)}$ in (1) with $e^{-j(\Delta\phi_{ij}+\Delta t_{ij}f)}$ to form the frequency-dependent matrices $\mathbf{C}_w(f)$ and $\mathbf{D}_w(f)$. The model parameters Δf_k, $\Delta\phi_{ij}$ and Δt_{ij} are the variable center frequency, phase shifts and phase delays respectively, and are functions of the physical length L and effective index n_{eff} of the waveguides. In the frequency domain, the model can be represented as follows

$$\hat{\mathbf{S}}_w(f, \Delta f_c, \Delta L, n_{eff}) = (\mathbf{C}_w(f)(j2\pi(f + \Delta f_k + \Delta f_c)\mathbf{I}_m - \mathbf{A})^{-1}\mathbf{B} + \mathbf{D}_w(f)) \quad (7)$$

where the parameter Δf_c is used to adjust the optical carrier frequency f_{cs} of the simulation. While not discussed in this work, leveraging the state-space representation and the time-delay property of the Laplace transform, the frequency-domain model (7) can be converted into a set of ordinary differential equations (ODEs) that can be adopted for time-domain simulations.

III. Application Example

In this numerical example, the frequency-domain modeling of a balanced Mach-Zehnder interferometer (MZI) is discussed. The layout of the MZI, comprising two directional couplers and two waveguides, is illustrated in Fig. 1. The center frequency is swept over one FSR from 192.7 THz to 194.1 THz by varying the length of the upper waveguide arm according to $\Delta L \in [67.8, 68.5]$ µm. The directional couplers are simulated in Lumerical FDTD whereas the waveguides are analytic models that take into account the linear dispersion. The scattering parameters of the entire device are evaluated in Luceda IPKISS over the frequency range [192.0; 194.9] THz at the center of the parameter range, i.e. L = 68.15 µm. Next, the scattering parameters are shifted to baseband using $f_c = 193.42$ THz. Following the CVF modeling procedure, a stable and passive CVF model is built with 13 poles, leading

to a maximum modeling error between the data and the model response below $-62.1\,\mathrm{dB}$.

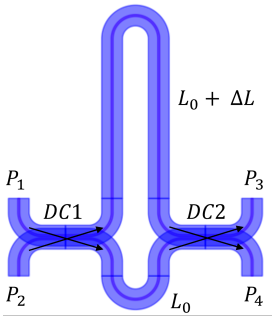

Fig. 1. Layout of the MZI.

By plugging the effective index of the linear dispersive waveguides in (6) and solving for f_k, it is possible to express Δf_k in terms of the waveguide length. The model parameters Δt_{ij} and $\Delta \phi_{ij}$ are derived from a physics-based analysis of the filter, but since their expressions are quite lengthy, they are not discussed here. Then, by taking the state-space matrices of the CVF model, and combining them with Δf_k, Δt_{ij} and $\Delta \phi_{ij}$, it is possible to build the wideband macromodel (7). In the results below, the optical carrier frequency is not varied, and Δf_c is fixed at 0.

Now that the model is computed, it can be used to predict the frequency response of the MZI, as illustrated in Fig. 2. It is important to note that the largest errors are expected at the edge of the design space, where the magnitude and phase response are mostly affected by the change of the center frequency. To illustrate this, the model accuracy, defined as the RMS error w.r.t. the simulation data, is evaluated for different values of ΔL, see Fig. 3. Although the model performance is reduced near the edges of the design space, it still achieves a reasonable accuracy which should generally suffice for most practical design and optimization applications. While not discussed here, time-domain simulation at arbitrary optical carrier frequency can be performed by solving the system of ODEs that can be derived from (7). Moreover, it is possible to convert the resulting system of ODEs in an equivalent SPICE netlist, as discussed in [5].

IV. Conclusion

In conclusion, the key strength of this parametric wideband macromodel lies in its capacity to attain accurate representations with a minimal set of expensive electromagnetic (EM) simulations, resulting in significant benefits in terms of compactness and simulation speed. Furthermore, the macromodel successfully captures the dispersive characteristics of the device, enabling precise and reliable simulations. Moreover, its flexibility to be simulated at multiple wavelengths enhances its applicability and practicality, making it a valuable tool for modeling and simulating WDM systems.

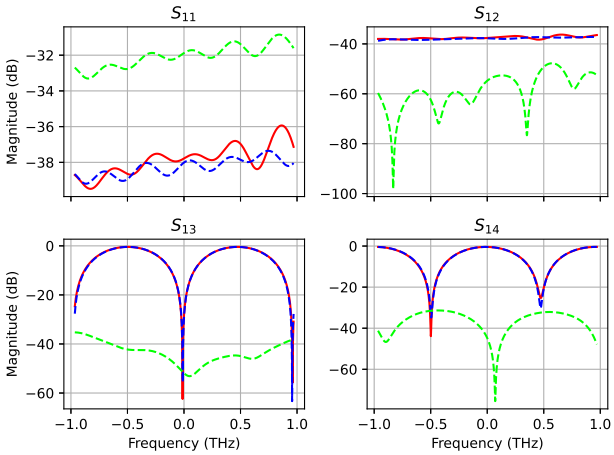

Fig. 2. The magnitude response of the wideband baseband macromodel (7), computed following the methodology outlined in this work, evaluated for $\Delta L = 67.8\,\mu\mathrm{m}$. The red solid line represents the simulated scattering parameters, the blue dashed lines represent the model, and the green line is the magnitude of the error between the two.

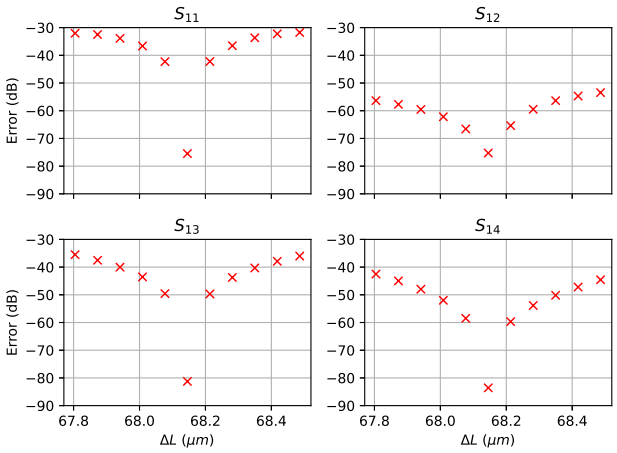

Fig. 3. RMS absolute error between the model and the simulated data for different values of ΔL.

References

[1] W. Bogaerts and L. Chrostowski, "Silicon Photonics Circuit Design: Methods, Tools and Challenges," *Laser & Photonics Reviews*, vol. 12, p. 1700237, Apr. 2018.

[2] S. Grivet-Talocia and B. Gustavsen, *Passive macromodeling: theory and applications*. Wiley series in microwave and optical engineering, Hoboken, New Jersey: John Wiley & Sons, Inc, 2016.

[3] Y. Ye, D. Spina, D. Deschrijver, W. Bogaerts, and T. Dhaene, "Time-domain compact macromodeling of linear photonic circuits via complex vector fitting," *Photonics Research*, vol. 7, p. 771, July 2019.

[4] D. Spina, Y. Ye, D. Deschrijver, W. Bogaerts, and T. Dhaene, "Complex vector fitting toolbox: a software package for the modelling and simulation of general linear and passive baseband systems," *Electronics Letters*, vol. 57, no. 10, pp. 404–406, 2021. _eprint: https://onlinelibrary.wiley.com/doi/pdf/10.1049/ell2.12116.

[5] Y. Ye, T. Ullrick, W. Bogaerts, T. Dhaene, and D. Spina, "SPICE-Compatible Equivalent Circuit Models for Accurate Time-Domain Simulations of Passive Photonic Integrated Circuits," *Journal of Lightwave Technology*, vol. 40, pp. 7856–7868, Dec. 2022.